ELSEVIER

Biophysical Chemistry 103 (2003) 1–11

Biophysical Chemistry

www.elsevier.com/locate/bpc

Effects of metabolites on the structural dynamics of rabbit muscle pyruvate kinase☆

Shaoning Yu, Lucy L.-Y. Lee, J. Ching Lee*

Department of Human Biological Chemistry and Genetics, University of Texas Medical Branch, Galveston, TX 77555-1055, USA

Received 28 January 2002; accepted 12 March 2002

Abstract

The activity of rabbit muscle pyruvate kinase (PK) is regulated by metabolites. Besides requiring the presence of its substrates, PEP and ADP, the enzyme requires Mg^{2+} and K^{+} for activity. PK is allosterically inhibited by Phe for activity. The presence of PEP or Phe has opposing effects on the hydrodynamic properties of the enzyme without an apparent change in secondary structure. In this study, the structural perturbation induced by ligand binding was investigated by Fourier transform infrared (FT-IR) spectroscopy. Furthermore, the structural dynamics of PK was probed by H/D exchange monitored by FT-IR. Substrates and activating metal ions induce PK to assume a more dynamic structure while Phe exerts an opposite effect. In all cases there is no significant interconversion of secondary structures. PEP is the most efficient ligand in inducing a change in the microenvironments of both helices and sheets so much so that they can be detected spectroscopically as separate bands. These results provide the first evidence for a differential effect of ligand binding on the dynamics of structural elements in PK. Furthermore, the data support the model that allosteric regulation of PK is the consequence of perturbation of the distribution of an ensemble of states in which the observed change in hydrodynamic properties represent the two extreme end states.

Keywords: Pyruvate kinase; Fourier transform infrared spectroscopy; Dynamics; Allostery

1. Introduction

Muscle pyruvate kinase (PK) enzyme activity is regulated by metabolites. Besides requiring the presence of its substrates, PEP/ADP, the enzyme needs also Mg^{2+} and K^{+} before any activity can be detected. Furthermore, PK is allosterically regulated by Phe, which serves as an inhibitor. In the presence of Phe, the observed steady-state kinetics deviate from a Michaelis–Menten relationship and exhibits sigmoidicity, the extent of which increases with increasing Phe concentration.

As a result of extensive steady-state kinetic, thermodynamic and structural studies, the simplest model that is consistent with all the data is a concerted allosteric model [1,2]. One of the major observations is that the binding of Phe causes a

Abbreviations: PK, pyruvate kinase; FT-IR, Fourier transform infrared spectroscopy; CD, circular dichroism; PEP, phosphoenolpyruvate; TKM buffer, 50 mM Tris, 72 mM KCl, 7.2 mM $MgSO_4$, pH 7.5.

☆ To Professor John Schellman whose pioneering work inspired a generation of scientists in investigating protein dynamics.

*Corresponding author. Tel.: +1-409-772-2281; fax: +1-409-772-4298.

E-mail address: jclee@utmb.edu (J. Ching Lee).

0301-4622/03/$ - see front matter © 2003 Elsevier Science B.V. All rights reserved.
PII: S0301-4622(02)00146-1

cooperative change in protein conformation, as monitored by difference sedimentation velocity [1], analytical gel chromatography [3] and small angle neutron scattering [4]. Binding of Phe induces PK to assume an expanded or asymmetric shape whereas binding of PEP would elicit an opposite effect, namely, a contraction or assumption of a more symmetric shape. Small angle neutron scattering data provide additional information. Length distribution analysis of the scattering data indicates that all these structural perturbations involve pronounced changes of interatomic distances between 80 and 110 Å. Using the α-carbon coordinates of crystalline cat muscle PK, a length distribution profile was calculated and it accounts for a scattering profile of the inactive, expanded form [4], an observation in total agreement with the sedimentation and filtration data [1,3]. Hence, results from neutron scattering, X-ray crystallography, sedimentation and analytical gel chromatography reveal a consistent structural model of inactive PK, as shown in Fig. 1. The crystallographic structure of muscle PK shows that such an enzyme molecule is composed of three major domains, one of which protrudes out into the solvent. This exposed domain, identified as domain B, forms a cleft with domain A adjacent to the active site. Domain B is attached to domain A by what appears to be a flexible hinge region.

Insights into the ligand-induced structural changes were acquired with the aid of computational chemistry. With the aid of computer modeling, the crystal structure was manipulated in order to effect changes that are consistent with the conformational change described by the solution scattering data. The computer modeling involves the rotation of the B domain relative to the A domain, leading to the closure of the cleft between these domains. These manipulations resulted in the generation of new sets of atomic α-carbon coordinates, which were utilized in calculation, the result of which compared favorably with the solution data [4]. Thus, the hydrodynamic and scattering data indicate that the active conformation of PK is more symmetric in shape with a closed cleft between A and B domains.

It is gratifying to note that the computer manipulation of the crystalline structure of PK can generate structural data that are consistent with the experimental scattering data. Nevertheless, a major assumption involved in this modeling is that there is *no* significant change in the secondary structure in these domains. At present there is no information to specifically address this issue and evidence is needed to test the validity of this assumption, although a recent crystallographic study of the S402P PK mutant indicate that domain movement can be correlated to the formation or breakage of the inter-subunit salt bridge between Asp 177 of domain B and Arg 341 of domain A [5]. Hence, a study was initiated to monitor the structure of

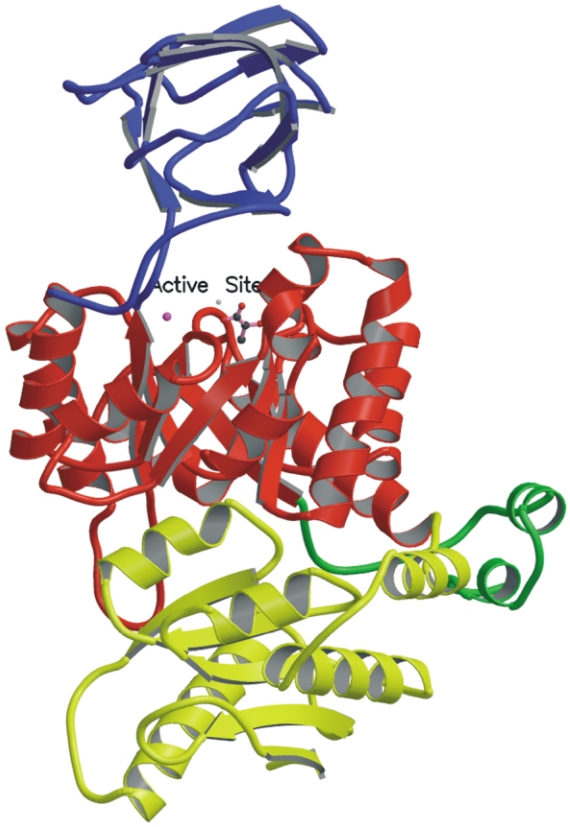

Fig. 1. Structure of rabbit muscle PK monomer. Each monomer consists of the N (green), A (red), B (blue) and C (yellow) domains. The active site is situated between the A and B domains. The structure is generated using the coordinates of Wooll et al. [5].

PK by CD and FT-IR in the presence of various metabolites. The dynamic motions that PK undergoes were studied by monitoring the rate of hydrogen exchange. Results of these studies show that metabolites do not induce any significant interconversion between secondary structures in PK, but do affect the dynamic motions of PK.

2. Experimental procedures

2.1. Materials

PK from rabbit muscle in 3.2 M $(NH_4)_2SO_4$ suspension, tricyclohexylammonium salt of PEP, disodium salt of ADP, NADH and lactate dilydrogenase type II were purchased from Boehringer Mannheim. The tricyclohexylammonium salt of PEP, Tris base, Tris–HCl, Phe were all obtained from Sigma Biochemical. KCl and $MgSO_4$ were purchased from Fisher. Deuterium oxide (99.96 atom% D) was the product of Cambridge Isotope Laboratories (Andover, MA). Sephadex G-25 fine was obtained from Pharmacia.

2.2. Methods

2.2.1. Circular dichroic study

The conformation of PK was monitored by CD using an AVIV Model 62D spectropolarimeter. The spectra were routinely recorded from 350 to 185 nm using a slit program yielding a 1.5-nm bandwidth at each wavelength. Overlapping spectra were obtained with the use of 0.01, 0.1 and 1.0 cm fused silica cells. A value of 109 was used for the mean residue weight in the calculation of ellipticities, $[\theta]$. All runs were performed at room temperature, i.e. approximately 23 °C. Six repetitive scans were taken for each experimental conditions and were averaged. Approximately, 0.5–1 mg/ml of PK was employed in each experiment.

2.2.2. FT-IR studies

Due to the high absorptivity of some ligands, CD is not the appropriate technique to monitor structural changes in PK induced by these ligands. Hence, FT-IR was chosen to monitor PK structure in the presence of Phe, PEP and ADP. The spectra of PK solutions at 10–13 mg/ml were obtained using a Bomem MB-Series FT-IR spectrometer (Quebec, Canada). For samples in H_2O and D_2O, a 7.5- or 50-μm spacer was used, respectively. In each case, 256 scans were obtained for each sample. The water-subtracted spectrum was obtained for the frequency region from 1800 to 1350 cm^{-1} and enhanced by Fourier deconvolution. The second derivative spectrum was calculated using a 7-point Savitsky–Golay derivative function. All curve fittings were performed with an iterative Gauss–Newton nonlinear regression program included in the operative software package provided by Bomem. The results of the deconvolution procedure were checked by reconstructing the observed spectrum from the resolved bands. It was assumed that the fraction of residues composing each secondary structural element is proportional to the relative percent area of the associated vibrational band.

2.2.3. PK sample preparations

The $(NH_4)_2SO_4$ precipitated rabbit muscle PK suspension was pelleted. The pellet was resuspended in 1 ml of buffer (either TKM or Tris) and dialyzed against 100 ml of the appropriate buffer for at least 12 h with three changes of buffer. The protein concentration was determined by absorbance at 280 nm, using an absorptivity of 0.54 ml/mg cm [1]. In preparing PK samples in the presence of PEP, ADP and Phe, 10 μl of a 20-mM solution of ligand was added to 100 μl of the dialyzed PK solution, which was then lyophilized. 100 μl H_2O was added to the lyophilized sample to resuspend the sample.

Fully deuterated samples were prepared in the same way except that D_2O was added. In addition, the PK lyophilized samples were resuspended in D_2O for 48 h, lyophilized and resuspended in D_2O again before FT-IR spectra were collected.

2.2.4. H/D exchange

One-hundred microlitres of D_2O was added to the lyophilized PK sample which was initially in H_2O buffer. FT-IR spectra were collected within 1 min of solubilization of the sample. Eight scans were collected for each time interval between 1 and 10 min while 16 and 32 scans were collected for each time interval between 11 and 60 min and longer, respectively.

2.2.5. Calculation of amide proton exchange rate

The fraction of unexchanged amide proton, X, was calculated at various time intervals using Eq. (1)

$$X = (A_{II} - A_{II\infty})/A_I\omega \quad (1)$$

where A_I and A_{II} are the absorbance maximum of the amide I and II bands, respectively. $A_{II\infty}$ is the amide II absorbance maximum of fully deuterated PK; and ω is the ratio of A_{IIo}/A_{Io}, with A_{IIo} and A_{Io} being the respective absorbance maximum for the amide II and amide I bands of PK in H_2O [8].

2.2.6. Enzyme kinetics

The enzymatic activity of PK was determined by the lactate dehydrogenase coupled enzyme assay [9] in TKM buffer containing 0.3 mM NADH and 10 μg/ml lactate dehygrogenase. The concentration of ADP in the assay mixture was fixed at 2 mM while PEP was the variable substrate.

3. Results

The ability of PK to replace its exchangeable protons was monitored by amide proton exchange kinetics. A preliminary experiment using tritium exchange indicated that PK undergoes rapid exchange during the initial 30 min and the rate approaches a slow phase after 60 min. Substrate and inhibitor affected the kinetics of proton exchange. These changes in the tritium exchange kinetics may originate from a change in the dynamic behavior of the protein, a change in surface of the protein exposed to solvent or a change in the secondary or tertiary structure of the protein leading to a change in dynamics or surface exposure.

Since global tritium exchange kinetics as monitored in these preliminary experiments do not distinguish among these possible mechanisms, spectroscopic techniques were employed to provide additional insights. The presence of high concentrations of ligands with high absorptivity obviates CD as a method to monitor changes in the secondary and tertiary structures of PK in the presence of 2 mM PEP, ADP or 12 mM Phe. Hence, FT-IR was employed. This spectroscopic technique has another advantage of being able to monitor the β-turns, β-sheets and α-helices directly. Since the sample preparation for FT-IR measurements included lyophilization of PK, it is essential to demonstrate the retention of structural integrity of PK after such treatment. Enzyme kinetics was employed to compare the behavior of PK before and after lyophilization. Fig. 2 shows the kinetic behavior of PK with PEP as the variable substrate. It is evident that the kinetic behavior of PK has not been affected by lyophilization and resuspension since the semi-log plots of velocity vs. $-\log(\mathrm{PEP})$ are identical. In both cases the K_m for PEP was 52 μM. In addition, the long procedure to achieve full deuteration of PK did not elicit any detrimental effects. Hence, results of this study reflect the behavior of the native PK.

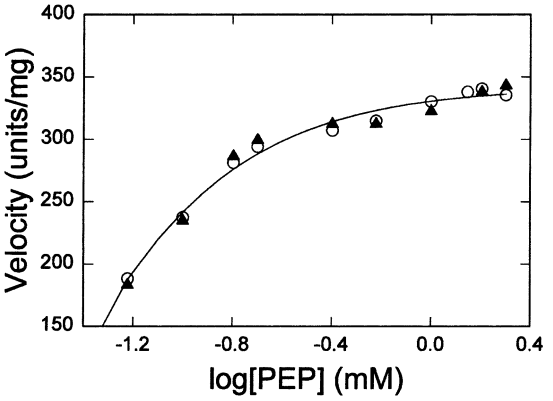

Fig. 2. Steady-state kinetics of PK before (○) and after (▲) lyophilization. PEP was the variable substrate in the presence of 2 mM of ADP.

The averaged, triplicate IR absorption spectrum of PK in 50 mM Tris, at pH 7.5 and 23 °C is shown in Fig. 3A. The variations observed in the absorbance spectra most likely were due to experimental uncertainties in subtracting the H_2O background. Control experiments showed that although the intensities may vary, the band wave numbers of the second derivative spectra were not altered. The second derivative spectrum was calculated as described by Susi and Byler [6]. Curve-fitting was performed with an iterative Gauss–Newton nonlinear regression program [7]. The spectrum exhibited bands corresponding to β-sheet ($\sim$1635 cm^{-1}),

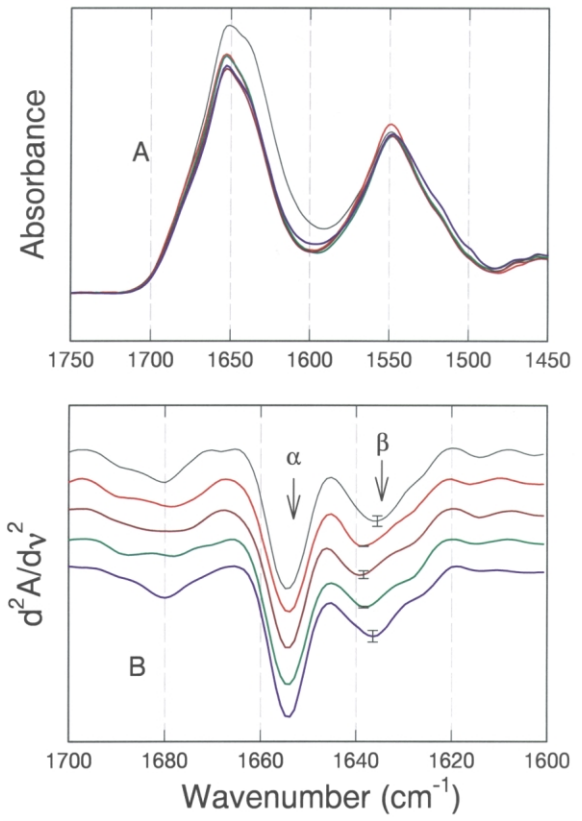

Fig. 3. FT-IR spectra of PK in H_2O. (A) Averaged, triplicate absorption spectra of the amide I and II regions. (B) Second-derivative amide I spectra. The bar represents the maximum deviations. The spectra are displaced in the *Y*-axis for clarity in presentation. The solution composition and color of the line are: (black) Tris buffer; (red) TKM buffer; (green) 2 mM PEP in TKM buffer; (dark red) 2 mM ADP in TKM buffer; (blue) 10 mM Phe in TKM buffer.

α-helix (~1656 cm^{-1}) and β-turns (1680 cm^{-1}), as shown in Fig. 3B. Quantitative analysis by curve-fitting shows that rabbit muscle PK consists of 37% β-sheet, 40% α-helix and 13% β-turns. These results are consistent with the structure of muscle PK defined by X-ray crystallography [5,10–12].

The effect of activating cations (K^+ and Mg^{2+}) was tested. Fig. 3A and B show the averaged absorption and second derivative spectrum, respectively, of PK in the presence of 72 mM K^+ and 7.2 mM Mg^{2+}. There are observable differences in the second derivative curve as compared with that in Tris buffer. The band corresponding to β-turns was resolved into bands at 1683 and 1673 cm^{-1}. The band at 1635 cm^{-1} was shifted to 1638 cm^{-1} and there is an appearance of a shoulder at approximately 1628 cm^{-1}. Curve-fitting resulted in a distribution of 20% β-turns, 42% α-helix and 32% β-sheets.

The effects of 2 mM PEP or ADP were tested and the results are shown in Fig. 3. Comparing these averaged triplicate spectra with that in TKM buffer, it is obvious that they resemble the spectra in TKM buffer although the spectral details between 1620 and 1640 cm^{-1} are different. In the presence of substrates the spectra were resolved into more prominent features, especially at 1630 cm^{-1}. These results indicate that no significant conversion between secondary structural elements

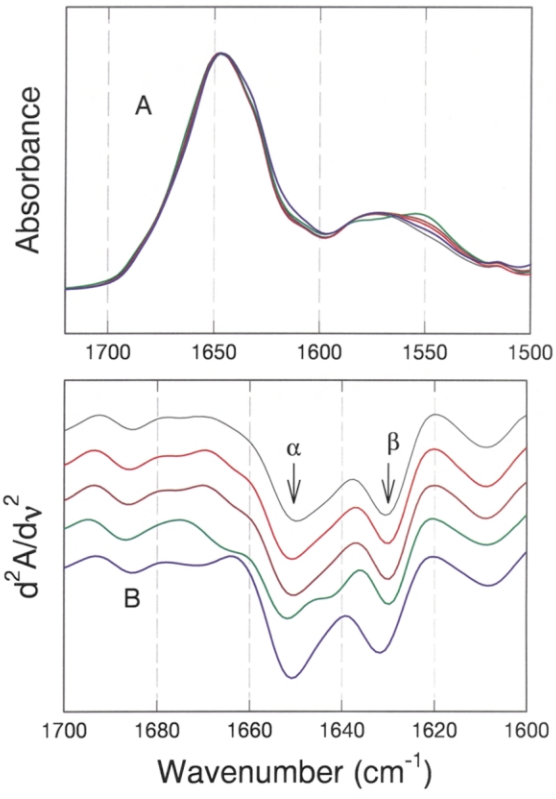

Fig. 4. FT-IR spectra of PK in D_2O. (A) Averaged absorption spectra of the amide I and II regions. (B) Second-derivative amide I spectra. The solution compositions and color codes are the same as in Fig. 3.

in PK are induced by the binding of the substrates, PEP or ADP, although some β-sheets are shifted to a different environment. Thus, qualitatively the activating metal ions and substrates elicit similar structural perturbation in PK.

The effect of 10 mM Phe was tested and the results are shown in Fig. 3. By comparing the spectra in Fig. 3, it is evident that there is no significant difference in the IR spectra for PK in the Tris buffer alone and in the presence of saturating amount of Phe. Tentatively, one may conclude that Phe does not induce significant secondary structural changes in PK, although the binding of Phe reverts the changes in the microenvironments of these secondary structures induced by the activating ions.

An equivalent set of FT-IR experiments were conducted in D_2O. Results are summarized in Fig. 4A and B. Effects of ligand binding on these FT-IR spectra are different from that in H_2O. The bands assigned to β-turns ($\sim$1680 cm^{-1}), α-helix ($\sim$1650 cm^{-1}) are all perturbed. The effect of activating metals on these spectra is not as obvious as that in H_2O. Phe induced an increase in the bandwidths at 1630 and 1650 cm^{-1}. An increase in bandwidth implies an increase in the heterogeneity of microenvironment surrounding these secondary structural elements. A decrease in bandwidth implies the opposite. Thus, the binding of Phe apparently induces heterogeneity in the microenvironments for both the β-sheets and α-helices. While the inclusion of ADP, one of the substrates, has no demonstrative effects on the IR spectrum, PEP induces a resolution of the band at $\sim$1650 cm^{-1} to two bands, namely, at $\sim$1653 and 1643 cm^{-1}. This result indicates that PEP perturbs the helical structures of PK so that there are at least two populations of helices with distinct microenvironments.

In summary, the studies of PK in H_2O and D_2O enhance the chance of detecting the structural perturbations due to ligand binding. H_2O and D_2O serve as environmental perturbations by altering the strength of hydrogen bonding [13–15].

The effect of activating cations (K^+ and Mg^{2+}) was also studied by CD in two buffer systems—Tris and phosphate. Six repetitive CD scans were taken for each experimental condition and are averaged. In Fig. 5A the averaged spectrum of PK in 50 mM Tris, pH 7.5 and 23 °C is shown. The dotted line represents the averaged spectrum of PK in Tris alone while the solid line shows that of PK in Tris buffer supplemented with 72 mM K^+ and 7.2 mM Mg^{2+}. It is evident that the presence of activating cations induces a change in the magnitude of ellipticity only, without significant shifts in fine features of the spectrum in both the near and far UV region. These results imply that CD detects no significant change in the secondary and tertiary structures of PK induced by the presence of activating cations. The change in the magnitude of ellipticity is most likely due to a change in the absorbance of the protein resulted from a perturbation of the rotational freedom of tryptophan [16].

Similar results are obtained in phosphate buffer as shown in Fig. 5B. The dotted and solid lines represent the averaged spectrum of PK in phosphate buffer alone and supplemented with activating cations, respectively.

In summary, these spectroscopic data indicate that the inclusion of activating cations and other ligands does not induce significant conversion between secondary structural elements in PK.

The effects of ligand binding on the dynamics of PK were monitored by D/H exchange as reflected in changes in the absorption spectra in FT-IR. The exchange procedure required re-solulilization by 100% D_2O of a lyophilized sample. FT-IR spectra were collected with regular intervals from 1 to 180 min. The second derivative spectra in the absence K^+ and Mg^{2+} were shown in Fig. 6A. In the absence of activating metal ions, the peak at 1635 cm^{-1} was shifted, almost immediately at the first time point of 1 min, to 1630 cm^{-1} with a concomitant change in intensity with time. These spectral changes are indications of the D/H exchange in the β-sheets. After 10 min of exchange, the band intensity and peak position have essentially reached their maximal changes. In addition, the spectral region between 1650 and 1640 cm^{-1} showed a complex pattern of change with time. Initially a shoulder was observed and with an increase in time of exchange it merged into the main band. The 1655 cm^{-1} band observed in H_2O shifted to lower wave number. The band

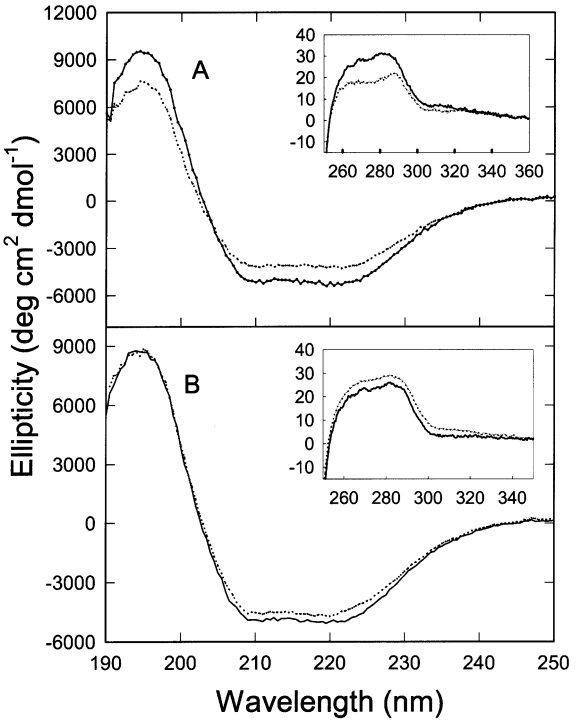

Fig. 5. CD spectra of PK in the absence and presence of activating metal ions, (A) in 50-mM Tris buffer at pH 7.5; (B) in 20-mM phosphate buffer at pH 7.5. The symbols and experimental conditions are: (–) with; (– –) without 72 mM KCl and 7.2 mM $MgSO_4$.

intensity decreased with increase in time of exchange, although there was approximately a 50% decrease even at the 1-min time point. The rate of decrease in intensity is a reflection of the exchange rate. The decrease in intensity at 1680 cm^{-1} was immediate, indicating a rapid exchange of amide protons in the β-turns of PK. The spectrum at the final time point remained constant for 4–5 days. The effects of K^+ and Mg^{2+} were shown in Fig. 6B. The basic pattern of exchange was retained. However, a larger change in intensity was observed even at the 1-min time point. These results imply that the activating metal ions induce an increase in number of rapidly exchangeable amide protons.

The presence of either PEP or ADP shows a pattern of exchange that is quite similar to each other (Fig. 6C and D). A very rapid exchange was observed in both the helices and sheets. There was a clear indication of the presence of two different populations of helices, as shown by the pattern of exchange between 1640 and 1660 cm^{-1}.

The change in the second derivative spectra reflecting the amide proton exchange in the presence of Phe is shown in Fig. 6E. Even at the 1-min time point there is an approximately less than 50% decrease in intensity in the band at 1650 cm^{-1} indicating that a significant amount of amide protons in the helices were exchanged very rapidly. The intensity then gradually decreases. There were slow exchange protons which were all apparently exchanged by 180 min. The exchange pattern in the band at $\sim$1630 cm^{-1} shows an attaining of final intensity almost instantaneously. This result implies that a fraction of β-sheets is exchanging very rapidly and the rest is not exchanging. Within the time frame of the experiment no exchangeable amide proton was detected in the β-sheets, an observation that differs from that of the helices.

The global exchange rate was extracted from the data with the aid of Eq. (1) and the results are shown in Fig. 7. In the absence of any ligands, a significant fraction of protons, approximately 75%, was exchanged already by the first measurable time point. It is interesting to note that binding of substrates, ADP and PEP, actually leads to a greater fraction of protons to be exchanged very rapidly ($\approx$80%). In the presence of Phe, the percentage of rapidly exchanged protons is intermediate. The rates of exchange after 10 min apparently are indistinguishable regardless of the nature of ligand present.

4. Discussion

An important feature of allosteric regulation is the communication between ligand binding sites and subunits of an oligomeric enzyme such as PK. One of the goals in this field is to elucidate the structural elements involved in this communication network and the pathway through which a particular allosteric effector transmit its signal. Based on the results of crystallographic studies of PK, it has been proposed that the structural changes involved in signal transmission are mainly reorientation of domains [17]. According to this proposed

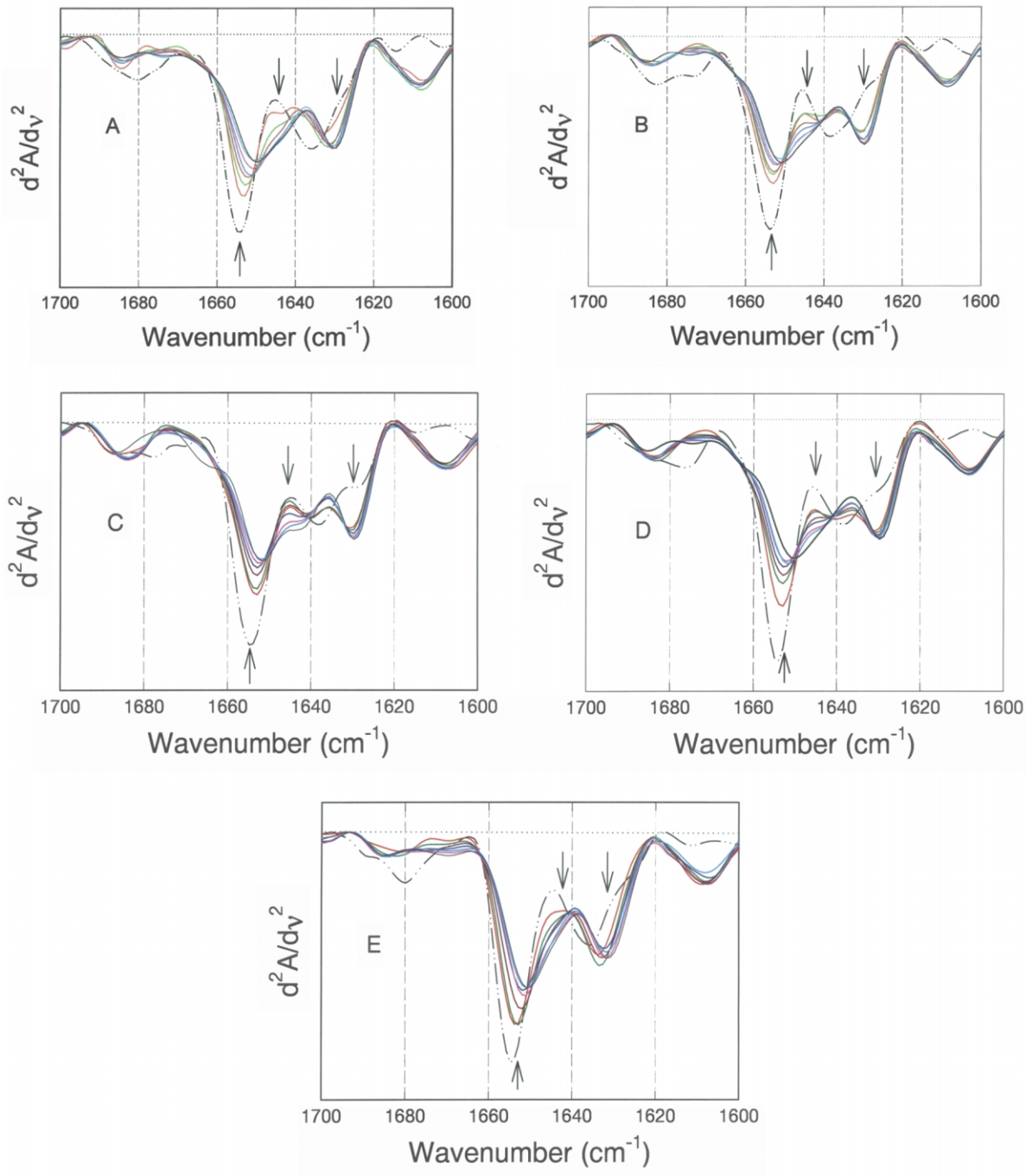

Fig. 6. Amide proton exchange as monitored by FT-IR. The spectra were recorded at 1, 10, 30, 60, 120, 180 min and 2 days after solubilization of a lyophilized PK sample. Arrows indicate the direction of shift in spectra with time. The symbols and spectra of PK (– •• –) in H_2O and (–) D_2O. (A) In Tris buffer; (B) in TKM buffer; (C) in 2-mM PEP–TKM buffer; (D) in 2-mM ADP–TKM buffer and (E) in 10-mM Phe–TKM buffer.

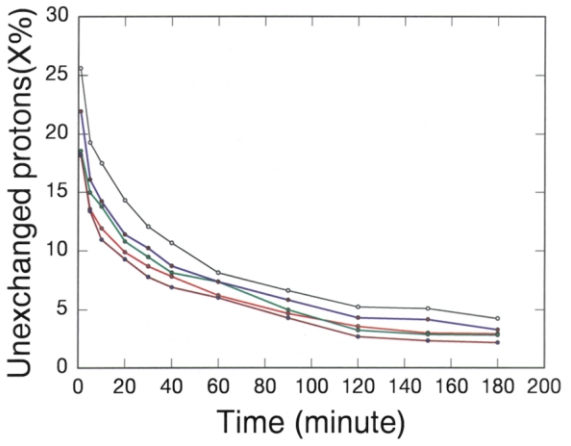

Fig. 7. Global amide proton exchange rate. The solution compositions and color codes are the same as in Fig. 3.

structural model, there is no significant interconversion in secondary structures. Crystallographic reports on PK–ligand complexes are consistent with the proposed model [18–20]. These structural data are also consistent with the 2-state model proposed as a result of global analysis of solution thermodynamic data [1,2]. A key feature of the 2-state model is that the enzyme exists as a product of an equilibrium between at least two states, each of which exhibits specific affinities towards various ligands [4]. The direct implication is that PK is present as an ensemble of states with active and inactive states representing the two extreme end states. However, it is difficult to detect the presence of such an ensemble of states by crystallography, although recently Wooll et al. [5] reported the detection of heterogeneity in the orientation of the B domain with respect to the A domain by crystallography. The freedom of rotation is linked to a single site mutation approximately 30–40 Å away. An ensemble of states may represent much subtle changes such as changes in dynamics. In order to provide insights in structural dynamics of PK, D_2O is employed in this study as a perturbation, in addition to ligands, of PK structures monitored by FT-IR.

Inclusion of D_2O provides a subtle perturbation of the dynamics of protein structure by strengthening the hydrogen bonding network. If the structural perturbation by ligand binding involves minor alterations in the energetics of interactions between structural elements instead of gross interconversion of secondary structural changes, then a change in hydrogen bonding energetics may be sufficient to assist in revealing these ligand-induced structural perturbations. In this study of rabbit muscle PK, the resolving power of FT-IR has provided the evidence for the differential effects of metabolites on the structural environments of helices and sheets.

In H_2O solutions, in which the hydrogen bonding is weaker, ligands induce significant changes in the spectral regions for β-sheets without any detectable changes in α-helices. These results imply that ligand bindings do not induce enough changes in energetics to alter the inter-helical bonding. Therefore, the spectral band at $\sim$1654 cm^{-1} remained the same in all the experimental conditions, with not even a change in bandwidth. In contrast, there is not only a significant perturbation in the spectral region associated with β-sheets, but also the nature of perturbation is linked to the specific ligand. In the presence of substrates and activating metal ions, the main band shifts to a higher wave number, $\sim$1638 cm^{-1}, and a clear resolution into a minor band at $\sim$1628 cm^{-1}. PEP binding causes the best resolution of the minor band. A shift to higher wave number implies a weakening of the inter-sheet or hydrogen bonding network. Thus, the binding of substrates and activating metal ions shifts PK to a structure which retains the relative distribution of the secondary structures but is probably more loosely packed. This loosening of structural packing should lead to a greater extent of amide protons to exchange rapidly, a prediction in total agreement with the results shown in Fig. 7. In the presence of the allosteric inhibitor Phe, an opposite effect on the spectral band for β-sheets is observed. The main band is shifted to $\sim$1636 cm^{-1}. This implies that the inter-sheet interaction is stronger and there is a decrease in the population of rapidly exchangeable amide protons, as shown in Fig. 7.

In D_2O solution, in which the hydrogen bonding is stronger, binding of ligands has no significant effects on the spectral region associated with β-sheets. Nevertheless, binding of the substrate PEP

induces a resolution of the spectral band for α-helices into two bands, ~1652 and ~1642 cm^{-1}. The combination of results in H_2O and D_2O indicate that PEP binding exerts the most significant perturbations to the microenvironments of all secondary structures in PK without inducing an interconversion between helices and sheets. Combining these spectral data with the hydrodynamic data conducted under similar conditions, the emerging view is that binding of PEP leads to an increase in the dynamics of the structure, a change that is also reflected in an alteration of the hydrodynamics of PK [3]. The binding of Phe yields spectral properties very similar to that of PK in just Tris buffer. Since the spectra of the Phe–PK complex were acquired in the presence of activating metal ions, this spectral result implies that Phe can overcompensate for the effects of activating metal ions. This observation is consistent with the results of hydrodynamic studies [1], namely, the Phe-induced change in sedimentation coefficient of PK is larger when the activating metal ions are present in the buffer solution. Thus, the Phe-induced structural changes in PK are in the opposite direction of PEP.

In summary, metabolites of PK exert significant perturbations in the structural dynamics of the enzyme. These subtle changes may not be detectable by X-ray crystallography. The challenge is to identify the structural elements whose microenvironment and dynamic behavior have been perturbed by these metabolites.

Acknowledgments

The preliminary studies by Suzanne Woodard, Bi-Hung Peng and Aichun Dong are greatly appreciated. This paper was supported by NIH Grant GM-45579 and the Robert A. Welch Foundation grants H-0013 and H-1238.

References

[1] R.W. Oberfelder, L.-Y. Lee, J.C. Lee, Thermodynamic linkages in rabbit muscle pyruvate kinase: kinetic, equilibrium, and structural studies, Biochemistry 23 (1984) 3813–3821.

[2] R.W. Oberfelder, B.G. Barisas, J.C. Lee, Thermodynamic linkages in rabbit muscle pyruvate kinase: analysis of experimental data by a two-state model, Biochemistry 23 (1984) 3822–3826.

[3] E. Heyduk, T. Heyduk, J.C. Lee, Global conformational changes in allosteric proteins: a study of *Escherichia coli* camp receptor protein and muscle pyruvate kinase, J. Biol. Chem. 267 (1992) 3200–3204.

[4] T.G. Consler, E.C. Uberbacher, G.J. Bunick, M.N. Liebman, J.C. Lee, Domain interaction in rabbit muscle pyruvate kinase: II small angle neutron scattering and computer simulation, J. Biol. Chem. 263 (1988) 2794–2801.

[5] J.O. Wooll, R.H.E. Friesen, M.A. White, et al., Structural and functional linkages between subunit interfaces in mammalian pyruvate kinase, J. Mol. Biol. 312 (2001) 525–540.

[6] H. Susi, M. Byler, Structure by Fourier transform infrared spectroscopy: second derivative spectra, Biochem. Biophys. Res. Comm. 115 (1983) 391–397.

[7] M. Byler, H. Susi, Examination of the secondary structure of proteins by deconvolved FTIR spectra, Biopolymers 25 (1986) 469–487.

[8] A.D. Barksdale, A. Rosenberg, Acquisition and interpretation of hydrogen exchange data from peptides, polymers, and proteins, Meth. Biochem. Anal. 28 (1982) 1–114.

[9] T. Bücher, G. Pfleiderer, Pyruvate kinase from muscle, Meth. Enzymol. 1 (1955) 435–440.

[10] T.M. Larsen, T. Laughlin, H.M. Holden, I. Rayment, G.H. Reed, Structure of rabbit muscle pyruvate kinase complexed with Mn^{2+}, K^+, and pyruvate, Biochemistry 33 (1994) 6301–6309.

[11] H. Muirhead, D.A. Clayden, D. Barford, et al., The structure of cat muscle pyruvate kinase, EMBO J. 5 (1986) 475–481.

[12] S.C. Allen, H. Muirhead, Refined three-dimensional structure of cat-muscle (M1) pyruvate kinase at a resolution of 2.6 A″, Acta Crystallogr. D52 (1996) 499–504.

[13] J. Hermans, H.A. Scheraga, The thermally induced configurational change of ribonuclease in H_2O and D_2O, Biochim. Biophys. Acta 36 (1959) 534–535.

[14] G.C. Kresheck, H. Schneider, H.A. Scheraga, The effect of D_2O on the thermal stability of proteins, J. Phys. Chem. 69 (1965) 3132–3144.

[15] G.I. Makhatadze, G.M. Clore, A.M. Gronenborn, Solvent isotope effect and protein stability, Nat. Struct. Biol. 2 (1995) 852–855.

[16] F.J. Kayne, C.H. Suelter, Effects of temperature, substrate, and activating cations on the conformations of pyruvate kinase in aqueous solutions, J. Am. Chem. Soc. 87 (1965) 897–900.

[17] A. Mattevi, G. Valentini, M. Rizzi, M.L. Speranza, M. Bolognesi, A. Coda, Crystal structure of *Escherichia coli* pyruvate kinase type I: molecular basis of the allosteric transition, Structure 3 (1995) 729–741.

[18] T.M. Larsen, M.M. Benning, G.E. Wesenberg, I. Rayment, G.H. Reed, Ligand-induced domain movement in

pyruvate kinase: structure of the enzyme from rabbit muscle with Mg^{2+}, K^{+}, and L-phospholactate at 2.7 Å resolution, Arch. Biochem. Biophys. 345 (1997) 199–206.

[19] T.M. Larsen, M.M. Benning, I. Rayment, G.H. Reed, Structure of the Bis (Mg^{2+})—ATP—oxalate complex of the rabbit muscle pyruvate kinase at 2.1 Å resolution: ATP binding over a barrel, Biochemistry 37 (1998) 6247–6255.

[20] M.S. Jurica, A. Mesecar, P.J. Heath, W. Shi, T. Nowak, B.L. Stoddard, The allosteric regulation of pyruvate kinase by fructose-1,6-bisphosphate, Structure 6 (1998) 195–210.